

Stability of Trions in Strongly Spin Polarized Two-Dimensional Electron Gases

S. A. Crooker

National High Magnetic Field Laboratory - LANL, MS E536, Los Alamos, NM 87545

E. Johnston-Halperin and D. D. Awschalom

Department of Physics, University of California, Santa Barbara CA 93106

R. Knobel and N. Samarth

Department of Physics, Pennsylvania State University, University Park PA 16802

(Submitted 5 January 2000)

Low-temperature magneto-photoluminescence studies of negatively charged excitons (X_s^- trions) are reported for n -type modulation-doped ZnSe/Zn(Cd,Mn)Se quantum wells over a wide range of Fermi energy and spin-splitting. The magnetic composition is chosen such that these magnetic two-dimensional electron gases (2DEGs) are highly spin-polarized even at low magnetic fields, throughout the entire range of electron densities studied (5×10^{10} to $6.5 \times 10^{11} \text{ cm}^{-2}$). This spin polarization has a pronounced effect on the formation and energy of X_s^- , with the striking result that the trion ionization energy (the energy separating X_s^- from the neutral exciton) follows the temperature- and magnetic field-tunable Fermi energy. The large Zeeman energy destabilizes X_s^- at the $\nu = 1$ quantum limit, beyond which a new PL peak appears and persists to 60 Tesla, suggesting the formation of spin-triplet charged excitons.

PACS numbers: 75.50.Pp, 78.55.Et, 71.35.Ji, 75.50.Cn

Magnetic two-dimensional electron gases (2DEGs) represent a relatively new class of semiconductor quantum structure in which an electron gas is made to interact strongly with embedded magnetic moments.¹⁻⁴ Typically, magnetic 2DEGs (and 2D hole gases) are realized in modulation-doped II-VI diluted magnetic semiconductor quantum wells in which paramagnetic spins (Mn^{2+} , $S = \frac{5}{2}$) interact with the confined electrons via a strong J_{s-d} exchange interaction.⁵ This interaction leads to an enhanced spin splitting of the electron Landau levels which follows the Brillouin-like Mn^{2+} magnetization, saturating in the range 10-20 meV by a few Tesla. Since the spin splitting can greatly exceed both the cyclotron ($\approx 1 \text{ meV/T}$) and Fermi energies, these magnetic 2DEGs consist largely of spin-polarized Landau levels, and serve as interesting templates for studies of quantum transport in the absence of spin gaps.¹ In addition, it has been recognized that this interplay between the cyclotron, Zeeman and Fermi energies may also be exploited in magneto-optical experiments to gain insights into the rich spectrum of optical excitations found in 2DEGs.⁴ The aim of this paper is to use strongly spin-polarized magnetic 2DEGs, containing a wide range of electron densities, to shed new light on the spin-dependent properties of negatively charged excitons (or trions).

Predicted in 1958 by Lampert⁶ and first observed by Kheng⁷ in 1993, the singlet state of the negatively charged exciton (the X_s^- trion) consists of a spin-up and spin-down electron bound to a single hole.⁴ The energy required to remove one of these electrons (leaving behind a neutral exciton X^0) is the X_s^- ionization energy ΔE_X , usually defined as the energy between X_s^- and X^0 features in optical studies. ΔE_X is small; typically

only $\sim 1 \text{ meV}$, $\sim 3 \text{ meV}$, and $\sim 6 \text{ meV}$ in GaAs-⁸, CdTe-⁷, and ZnSe-based⁹ 2DEGs respectively. The spin-singlet nature of the two electrons in X_s^- suggests that ΔE_X – and hence trion stability – should be sensitive to the Zeeman energy and spin-polarization of the 2DEG. Here, we explicitly study highly spin-polarized magnetic 2DEGs to establish empirical correlations between Zeeman energy and trion stability over a broad range of carrier densities. In particular, magneto-photoluminescence (PL) measurements demonstrate the striking result that ΔE_X follows the energy of the Fermi surface, which can be tuned independently from the Landau levels via the strong Zeeman dependence on temperature and applied field. The role of the Fermi and Zeeman energies in determining ΔE_X is studied for all carrier densities, and qualitative agreement with numerical calculations is found. The giant spin-splitting in these systems is found to reduce ΔE_X , eventually driving a rapid suppression of X_s^- by the $\nu = 1$ quantum limit, beyond which the formation of a new peak in the PL (which persists to 60T) may signify the formation of spin-triplet charged excitons.

These experiments are performed at the National High Magnetic Field Laboratory, in the generator-driven 60 Tesla Long-Pulse magnet and a 40T capacitor-driven magnet (with 2000 ms and 500 ms pulse duration, respectively), as well as a 20T superconducting magnet. Light is coupled to and from the samples via single optical fibers (200 μm or 600 μm diameter), and excitation power is kept below 200 μW . Thin-film circular polarizers between the fiber and sample permit polarization-sensitive PL studies. In the pulsed magnet experiments, a high-speed CCD camera acquires complete optical spectra every 1.5 ms, enabling reconstruction of the entire

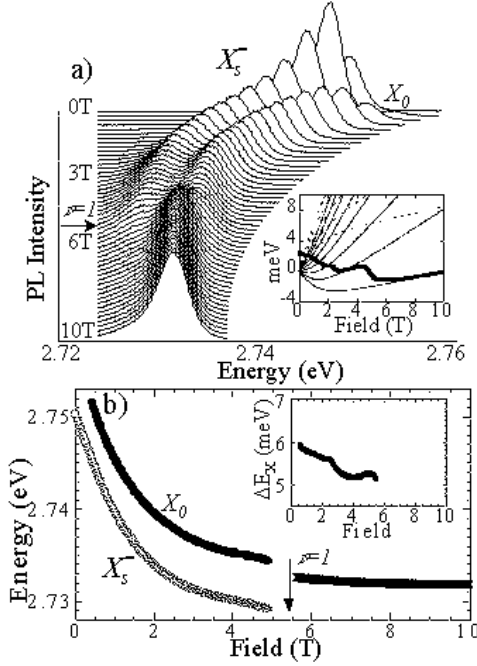


FIG. 1. a) Characteristic evolution of the PL spectra at 1.5K in low-density ($n_e = 1.24 \times 10^{11} \text{ cm}^{-2}$) magnetic 2DEGs, showing a collapse of the X_s^- and X_0 peaks at $\nu = 1$. Inset: spin-up (dotted) and spin-down (solid) LLs, and Fermi energy in this sample. b) PL peak energies. Inset: the $X_s^- - X_0$ energy splitting, which follows the Fermi energy.

spectra vs. field dependence in a single magnet shot.¹⁰ The magnetic 2DEG samples are MBE-grown n -type modulation-doped 105Å wide single quantum wells into which Mn^{2+} are “digitally” introduced in the form of equally-spaced fractional monolayers of MnSe . Specifically, the quantum wells are paramagnetic digital alloys of $(\text{Zn}_{1-x}\text{Cd}_x\text{Se})_{m-f}(\text{MnSe})_f$ with $x=0.1$ to 0.2 , $m=5$ and $f=1/8$ or $1/16$ effective monolayer thickness.¹ The electron densities, determined from Shubnikov-deHaas (SdH) oscillations in transport, range between 5×10^{10} and $6.5 \times 10^{11} \text{ cm}^{-2}$. All samples show a large spin splitting at 1.5 K, with “effective” g -factors in the range $70 < g_e^{eff}(H \rightarrow 0) < 100$.

Figure 1a shows the evolution of the PL spectra in a magnetic 2DEG with relatively low carrier density $1.24 \times 10^{11} \text{ cm}^{-2}$ and $g_{eff} = 73$ at 1.5K. This sample has a mobility of $14000 \text{ cm}^2/\text{Vs}$ and exhibits clear SdH oscillations in transport.¹¹ At $H = 0$, the data show a strong PL peak at 2.74 eV with a small satellite $\sim 6 \text{ meV}$ higher in energy. With applied field, the peaks shift rapidly to lower energy in the σ^+ polarization due to the large Zeeman energy (the σ^- emission disappears completely at low fields in all the magnetic 2DEGs, much like their undoped counterparts¹²). By 1 T, the satellite develops into a clear peak of comparable amplitude, and as will be verified in Fig. 2, we assign the high- and low-energy PL features to X_0 and X_s^- . At $\nu = 1$ (5.5 T), the smooth

evolution of the PL spectra changes abruptly as the X_s^- resonance collapses and a strong, single PL peak emerges at an energy between that of X_0 and X_s^- , as shown. This new PL feature persists to 60 T. Fig. 1b shows the energies of the PL peaks (the data are fit to Gaussians), where the discontinuity at $\nu = 1$ is clearly seen. The X_s^- ionization energy ΔE_X decreases and oscillates with magnetic field (inset, Fig 1b). Anticipating Figs. 3 and 4, we note that ΔE_X qualitatively mimics the Fermi energy in this low-density magnetic 2DEG (plotted in Fig. 1a, inset).

Owing to the giant spin splitting in this sample, the “ordinary” Landau level (LL) fan diagram for non-magnetic 2DEGs (with Landau levels evenly spaced by $\hbar\omega_c$, and spin splitting $\ll \hbar\omega_c$) is replaced by that shown in the inset of Fig. 1a. The LLs are simply calculated as

$$\varepsilon_{l,s} = \hbar\omega_c(l + \frac{1}{2}) + sE_Z B_{5/2}(5g_{Mn}\mu_B H / 2k_B T^*) \quad (1)$$

where l is the orbital angular momentum index and s is the electron spin ($\pm \frac{1}{2}$). Here, $\hbar\omega_c = 0.83 \text{ meV/T}$ is the electron cyclotron energy, and the second term is the Zeeman energy: $B_{5/2}$ is the Brillouin function describing the magnetization of the $S = \frac{5}{2}$ Mn^{2+} moments, E_Z is the saturation value of the electron splitting, $g_{Mn}=2.0$, and T^* is an empirical “effective temperature” which best fits the low-field energy shifts.⁵ We ignore the much smaller contribution to the Zeeman energy arising from the bare electron g -factor. At low fields, the spin-down LLs (solid lines) are Zeeman-shifted well below the spin-up LLs (dotted lines), leading to a highly spin-polarized electron gas - *e.g.*, by 1T, over 95% of the electrons are oriented spin-down in this sample. The Fermi energy ε_F (thick line) is calculated numerically by inverting the integral

$$N_e = \int_{-\infty}^{\infty} g[\varepsilon, B, T] f[\varepsilon, \varepsilon_F, T] d\varepsilon. \quad (2)$$

Here, N_e is the known electron density, $f[\varepsilon, \varepsilon_F, T]$ is the Fermi-Dirac distribution and $g[\varepsilon, B, T]$ is the density of states, taken to be the sum of Lorentzian LLs¹³ of width $\Gamma = \hbar/2\tau_s$ centered at the energies $\varepsilon_{l,s}$ given in Eq.1. The electron scattering time τ_s is obtained from analyzing SdH oscillations, or alternatively from the measured mobility.

Typically, identification of X_0 and X_s^- relies on their polarization properties in reflection or absorption^{4,7}-measurements which directly probe the available density of states. However in these magnetic 2DEGs, the huge Zeeman splitting and the relatively broad spectral linewidths (resulting from the high Mn^{2+} concentration) complicate these standard analyses. While reflectivity studies in these samples *do* confirm the presence of two bound states at zero field (as expected for X_0 and X_s^-), we rely on spin-polarized PL excitation measurements to verify the peaks in finite field, shown in Fig. 2. At fixed field and temperature, we record the PL while tuning the

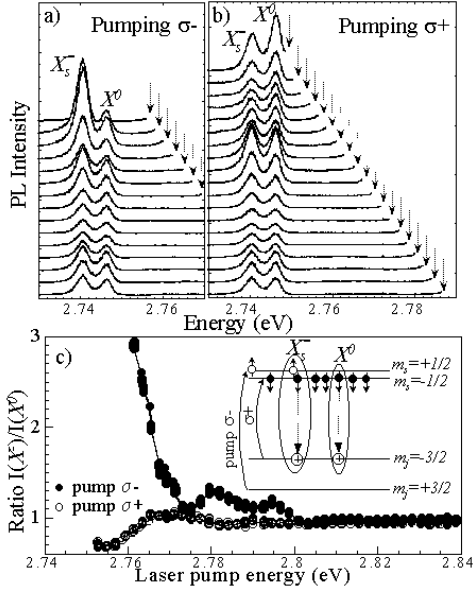


FIG. 2. a) PL-excitation at 2.2K and 1 T, showing an enhancement of X_s^- when injecting spin-up electrons on the σ^- resonance. b) A similar enhancement of the X^0 peak when injecting spin-down electrons. c) The intensity ratio $I(X_s^-)/I(X^0)$, with a schematic of the energy levels and processes involved (the light holes are split off due to quantum confinement effects).

energy and helicity of the excitation laser (a frequency-doubled cw Ti:Sapphire laser). Since the PL is entirely σ^+ polarized, it must arise from the recombination of a spin-down ($m_s = -\frac{1}{2}$) electron with a $m_j = -\frac{3}{2}$ valence hole (see diagram, Fig. 2c). If that $m_s = -\frac{1}{2}$ electron is part of an X_s^- trion, emission will occur at the X_s^- energy. Thus the probability of forming X_s^- is related to the number of spin-up ($m_s = +\frac{1}{2}$) electrons present in the system. By specifically injecting spin-up electrons at the σ^- resonance, we do indeed observe an enhancement of the X_s^- intensity (Fig. 2a). In contrast, injecting spin-down electrons with σ^+ light can (and does) only favor the X^0 intensity (Fig. 2b). The amplitude ratio, $I(X_s^-)/I(X^0)$, is plotted in Fig. 2c, where the effects of pumping spin-up and spin-down electrons are more easily seen. Of related interest, no difference in this ratio is observed when exciting above the ZnSe barriers (2.8 eV) - evidence that the injected spin is scrambled when the electrons spill into the well from the barrier regions.

With the aid of the diagram in Fig. 2c, the evolution of the PL spectra in Fig. 1 may be interpreted as follows: X_s^- and X^0 are competing channels for exciton formation, with X_s^- dominating at zero field. With small applied field, the large spin-splitting drives a rapid depopulation of the spin-up electron bands, reducing the probability of X_s^- formation and thus increasing X^0 formation, as observed. With increasing field and Zeeman energy, X_s^- continues to form until it is no longer ener-

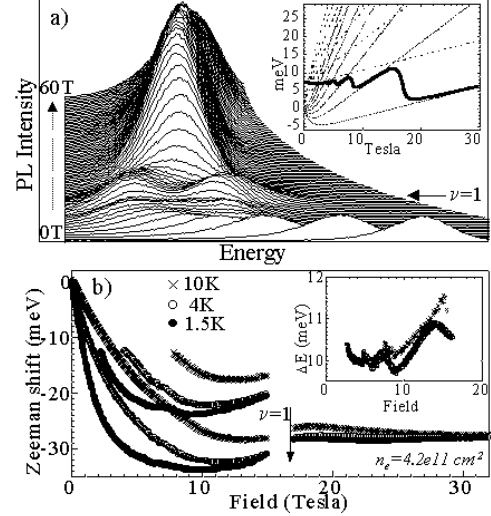


FIG. 3. a) Characteristic evolution of the PL spectra in high-density magnetic 2DEGs, with calculation of the LLs and Fermi energy (inset). b) Energies of the observed PL peaks at different temperatures, with the X_s^- - X^0 energy splitting (inset).

getically favorable to bind a spin-up electron - in this case, evidently, at $\nu = 1$ when the Fermi energy falls to the lowest LL. The PL peak which forms at $\nu = 1$ (and persists to 60T), with an energy *between* that of X_s^- and X^0 , represents formation of a stable new ground state. A likely candidate is the spin-triplet state of the negatively charged exciton (X_t^-), wherein both bound electrons are oriented spin-down. The X_t^- trion, predicted to become the ground state in nonmagnetic 2DEGs at sufficiently high magnetic field¹⁴, may also form stably in highly spin-polarized magnetic 2DEGs due to Zeeman energy considerations, although no theoretical description of these effects exists at present.

We turn now to results from high-density samples. Fig. 3 shows PL spectra and energy shifts observed in a high-density magnetic 2DEG ($n_e = 4.3 \times 10^{11} \text{ cm}^{-2}$, mobility = 2700 cm^2/Vs , and $g_e^{eff}(H \rightarrow 0) = 95$ at 1.5K). These data are characteristic of that obtained in samples with n_e up to $6.5 \times 10^{11} \text{ cm}^{-2}$, the highest density studied. Again, we observe a dominant PL peak at $H = 0$ which shifts rapidly down in energy with applied field. However, in contrast with the low-density 2DEGs, the high-energy satellite peak does not appear until 2 Tesla (at 1.5K). This satellite grows to a peak of comparable amplitude by 12 Tesla, and exhibits similar sensitivity to the energy and helicity of the pump laser as seen in Fig 2; therefore we again assign these features to X_s^- and X^0 . At $\nu = 1$ (17 Tesla), these resonances collapse and are again replaced by a strong emission at an intermediate energy which persists to 60T. The energy of the observed PL peaks at 1.5K, 4K, and 10K are plotted in Fig. 3b, along with ΔE_X (inset). Several features are notable. First, the X^0 peak only becomes visible at a

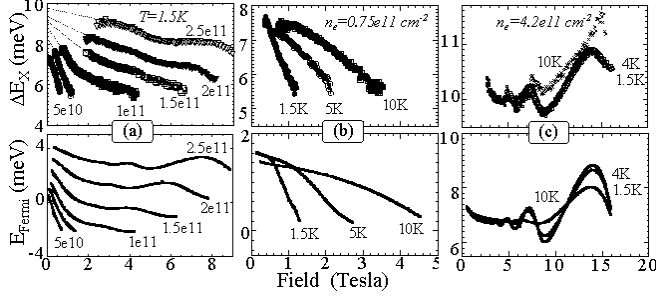


FIG. 4. Explicit dependence of the trion ionization energy ΔE_X on (a) carrier density in otherwise identical magnetic 2DEGs, and on temperature in b) low- and c) high-density samples, all showing marked similarity to numerical calculation of the Fermi energy.

particular *spin splitting* – not field – in support of the assertion that X^0 forms readily only when the spin-up electron subbands depopulate to a particular degree. In addition, the collapse of the X^0 and X_s^- peaks occurs at $\nu = 1$ independent of temperature, again indicating that the drop of the Fermi energy to the lowest LL destabilizes X_s^- . Finally, ΔE_X again follows the calculated Fermi energy in this sample, exhibiting oscillations in phase with the Fermi edge.

This latter behavior is unexpected but appears to be true in all of our samples. In contrast with studies in nonmagnetic 2DEGs, these data clearly demonstrate the relevance of both the Zeeman energy and the Fermi energy in determining the trion ionization energy ΔE_X . In Figure 4 we explicitly study this behavior and reveal the surprising result that ΔE_X closely follows the energy of the Fermi surface *regardless* of electron density, temperature, and applied field. Fig. 4a shows the measured field dependence of ΔE_X in six magnetic 2DEGs with electron densities from $n_e \approx 5 \times 10^{10}$ to $\approx 2.5 \times 10^{11} \text{ cm}^{-2}$. The data are plotted from the field at which distinct X^0 and X_s^- PL peaks first appear, until the collapse of the PL spectra. ΔE_X is seen to decrease rapidly with field at the lowest densities, but remain roughly constant and exhibit weak oscillations at high densities. Further, a rough extrapolation (dotted lines) reveals that ΔE_X at zero field increases from $\sim 7 \text{ meV}$ to 10 meV with carrier density. Aside from a $\sim 7 \text{ meV}$ difference in overall magnitude, these features are qualitatively reproduced by the numerical computation of the Fermi energy in these samples, plotted in the lower graph. It is natural to associate 7 meV with the “bare” ($n_e \rightarrow 0$) X_s^- binding energy, in reasonable agreement with earlier studies in low-density, nonmagnetic ZnSe-based 2DEGs.⁹ Thus, at least at zero field, ΔE_X reflects the “bare” X_s^- binding energy *plus* the Fermi energy, in agreement with a recent viewpoint¹⁵ wherein the ionization process requires removing one electron from X_s^- to the top of the Fermi sea.

In nonzero field, the Zeeman energy reduces the X_s^- ionization energy. The explicit temperature dependence of ΔE_X in the low-density magnetic 2DEG is particularly telling (Fig. 4b): Here, the small Fermi energy should play a minimal role ($\varepsilon_F \sim 1.5 \text{ meV} \ll 9 \text{ meV}$ total spin splitting), and the data should directly reveal the X_s^- ionization energy. At different temperatures, ΔE_X decreases from its zero-field value of $\sim 7.5 \text{ meV}$ at a rate which depends on the Brillouin-like spin splitting. In this sample, the 2DEG is almost immediately completely spin-polarized – no gas of “spin-up” electrons remains – and thus the drop in ΔE_X must reflect the influence of the Zeeman energy. Physically, the energy of the spin-up electron in X_s^- increases with spin splitting, becoming more weakly bound, reducing ΔE_X by roughly half of the total Zeeman splitting until the X_s^- destabilizes. Within this scenario, however, the rolloff in the slope of the data towards zero field is puzzling, possibly indicating that the energy *between* the Fermi edge and the spin-up subbands (rather than the Zeeman energy itself) may be the relevant parameter, as the calculated Fermi energy shows precisely the same behavior. No theoretical framework for this behavior exists at present. Alternatively, Fig 4c shows typical data from the high electron density sample where the Fermi energy (7.7 meV) is comparable to the total spin splitting (12.6 meV). Here, the measured ΔE_X clearly follows the oscillations of the calculated Fermi energy, with no clear indication of the role played by the Zeeman energy. We pose these questions for future theoretical models for X_s^- formation, which must necessarily include the Zeeman energy and the influence of a finite Fermi energy.

In conclusion, we have presented a systematic study of charged exciton formation in strongly magnetic 2DEGs, wherein the giant spin splitting dominates the cyclotron energy and the electron gas is highly spin-polarized. The trion ionization energy ΔE_X tracks the energy of the Fermi edge regardless of electron density, temperature or applied field, highlighting the important roles played by both the Fermi- and Zeeman energies. With increasing electron density, the data suggest that ΔE_X – at least at zero magnetic field – reflects the “bare” X_s^- ionization energy of $\sim 7 \text{ meV}$ *plus* the Fermi energy. Studies in low density samples show that the “bare” X_s^- binding energy is reduced by an amount proportional to the Zeeman energy, and in high density samples ΔE_X follows the oscillations of the Fermi surface as it moves between Landau levels. Quantitative interpretation of these data must await a more complete theory of X_s^- formation in electron gases. This work is supported by the NHMFL and nsf-dmr 9701072 and 9701484.

¹ I. P. Smorchkova, N. Samarth, J. M. Kikkawa, D. D.

- Awschalom, Phys. Rev. B, **58** R4238 (1998); *ibid* Phys. Rev. Lett., **78**, 3571 (1997).
- ² M.S. Salib *et al.*, Phys. Rev. B, **57**, 6278 (1998); J.X. Shen *et al.*, Surf. Sci., **361/362**, 460 (1996); F. J. Teran *et al.*, Physica B, **256-258**, 577 (1998).
- ³ A. Haury *et al.*, Phys. Rev. Lett., **79**, 511 (1997).
- ⁴ T. Wojtowicz *et al.*, Phys. Rev. B **59** R10437 (1999).
- ⁵ D. D. Awschalom and N. Samarth, J. Mag. Magn. Mater., **200**, 130 (1999).
- ⁶ M. A. Lampert, Phys. Rev. Lett. **1**, 450 (1958).
- ⁷ K. Kheng *et al.*, Phys. Rev. Lett, **71**, 1752 (1993); N. Paganotto *et al.*, Phys. Rev. B, **58**, 4082 (1998); R. T. Cox *et al.*, Acta Phys. Pol. A, **94**, 99 (1998)
- ⁸ A. J. Shields *et al.*, Adv. in Phys. **44**, 47 (1995); G. Finkelstein, H. Shtrikman, and I. Bar-Joseph, Phys. Rev. Lett, **74**, 976 (1995).
- ⁹ G.V. Astakhov , Phys. Rev. B, **60**, R8485 (1999); K. Kheng *et al.*, Superlattices and Microstructures, **15**, 253 (1994).
- ¹⁰ S. A. Crooker *et al.*, Phys. Rev. B, **60**, R2173 (1999).
- ¹¹ R. Knobel, N. Samarth, S. A. Crooker, and D. D. Awschalom, Physica E (in press).
- ¹² S. A. Crooker *et al.*, Phys. Rev. Lett., **75**, 505 (1995).
- ¹³ A. Potts *et al.*, J. Phys.: Cond. Matter, **8**, 5189 (1996).
- ¹⁴ A. J. Shields, M. Pepper, M. Y. Simmons, and D. A. Ritchie, Phys. Rev. B, **52**, 7841 (1995); D. M. Whittaker and A. J. Shields, Phys. Rev. B, **56**, 15185 (1997).
- ¹⁵ V. Huard *et al.*, Phys. Rev. Lett., **84**, 187 (2000); P. Hawrylak, Phys. Rev. B, **44**, 3821 (1991).